Electrically Addressing a Molecule–Like Donor Pair in Silicon: An Atomic Scale Cyclable Full Adder Logic†

ARTICLE *in* THE JOURNAL OF PHYSICAL CHEMISTRY C · JANUARY 2012

Impact Factor: 4.77 · DOI: 10.1021/jp103524d

Electrically Addressing a Molecule-Like Donor Pair in Silicon: An Atomic Scale Cyclable Full Adder Logic†

Yonghong Yan,‡ J. A. Mol,§ J. Verduijn,§ S. Rogge,§ R. D. Levine,*,∥,⊥ and F. Remacle*,‡,#

Departement of Chemistry, B6c, University of Liège, B4000 Liège, Belgium, Kavli Institute of Nanoscience, Delft University of Technology, Lorentzweg 1, 2628 CJ Delft, The Netherlands, The Fritz Haber Research Center for Molecular Dynamics, The Hebrew University of Jerusalem, Jerusalem 91904, Israel, and Department of Chemistry and Biochemistry and Department of Molecular and Medical Pharmacology and Crump Institute for Molecular Imaging, The University of California—Los Angeles, Los Angeles, California 90095

Received: April 19, 2010; Revised Manuscript Received: July 14, 2010

Electrical spectroscopy of a heteroatomic molecule-like shallow-donor pair in silicon can switch the molecule between two ionic states of opposite polarities. We study this charge reorganization theoretically by solving the time-dependent Schroedinger equation on a grid using an effective mass model. The ability to control the charge reorganization by applying external electrical fields is then used to design a cyclable full-adder that operates as a nonlinear finite state machine. The logic operations, equivalent to 32 switches, are implemented by realistic pulse voltages that induce diabatic and adiabatic charge transfer between the wells of the two donors. A RF-SET is used for the read out by charge detection.

1. Introduction

Logic circuits of reduced dimensions and of low power requirements that can be repeatedly cycled are of central current interest and activity. For recent discussions of devices that can operate on the molecular scale see ref 1 and refs therein. Here we suggest a design for a circuit of some complexity, namely, a full adder where all these aims can be realized in a two adjacent dopant atoms embedded in Si, either lithographically implanted[2] or randomly present in a Fin-FET transistor.[3] The simulation and some of the proposed physics is validated by our previous work[4] on a one dopant atom device that can be experimentally realized.[5] The difference is that here we use the pair of near neighboring dopant atoms to define a molecule-like system and the logic is implemented by our ability to control the electronic states of this molecule and measure the charge on each dopant at different field strengths.

When designed using a switching network,[6] a full adder requires the concatenation of two subunits, each of which is a half adder. It is therefore a circuit that requires a significant number (32) of switches to be implemented. The point of our recent work is to implement complex logic circuits on a single atom or molecule. We have previously analyzed an experimental system whereby a full adder can be realized by optical addressing[7] of one or two molecules. The operation of such a circuit can be simulated via kinetic equations.[8] The density of active quantum states in the present device is far lower. It is a two-center molecule embedded in Si and so it cannot vibrate or rotate. Except for the long time coupling to phonon modes,[9] the only degrees of freedom are electronic and so a quantum simulation is possible. The well-studied STIRAP (Stimulated Raman Adiabatic Passage) optical spectroscopy[10] is another quantum route that we suggested toward a full adder.[7a] A key element in the logic device that we propose here is the electrical addressing of the Si embedded device. Electrical addressing has the advantages that the energy loss per computation is low and a Si FinFET transistor device is potentially nearer to a real technology. The essential basic physics that we used has a similarity to the STIRAP optically addressed device[7a] except that here only two electronic states are needed. From the point of view of computer architecture, one can also regard the device proposed here as an example of a nonlinear finite state machine.[11] In this paper we restrict attention to Boolean variables with the usual meaning of variables that can assume only two values, e.g., 0 and 1. We are also interested in finite state machines where the variables are multivalued because the computational efficiency is then higher; see, e.g., ref 12.

2. Model for a Two Donor Dopant Molecule

The physical system we consider is a single electron bound to a shallow-donor pair (e.g., P_2^+) in silicon, subject to a time-dependent electric field that controls the localization of the charge on one or the other dopant atom. In principle, the electric field can be applied parallel or perpendicular to the $Si-SiO_2$ (001) interface. We discuss here the case where the electric field is applied parallel to the interface, using a source and a drain electrode. Figure 1 shows a schematic of the structure. Results when the field is applied perpendicular to the interface are reported in the Supporting Information, Figure S4.

Similar configurations have been proposed previously,[9,13] mostly in the context of the realization of qubits for quantum computing.[14] Most quantum-computation schemes rely on the spin states of a donor-bound electron or of the donor nucleus. For the actual readout a so-called "spin-to-charge" conversion is typically used, where only charge detection and no direct spin detection is needed; see, for example, ref 15 and, for a review, ref 16. While our aim here is to implement a classical full addition logic device, the implementation of a controlled charge transfer between two donor atoms by voltage pulses

† Part of the "Mark A. Ratner Festschrift".

* Corresponding authors. F.R.: e-mail, fremacle@ulg.ac.be; phone, +32 4 3662347; fax+32 4 3663413. R.D.L.: e-mail, rafi@fh.huji.ac.il; phone, +972 2 6585260; fax, +972-2-6513742.

‡ University of Liège.

§ Delft University of Technology.

∥ The Hebrew University of Jerusalem.

⊥ The University of California—Los Angeles.

Director of Research, FNRS, Belgium.

10.1021/jp103524d

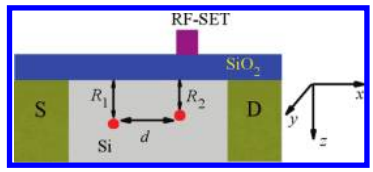

Figure 1. Schematic of the structure: two donor atoms are placed at the depths R_1 and R_2 (along the z direction) from the Si−SiO_2 interface and separated by a distance $d = |x_1 - x_2|$ in the x direction. The two electrodes, marked S and D, are used to apply an electric field along the x direction. The RF-SET used to detect the charge on the right dopant atom is also shown. See section 4 of the Supporting Information for results when the field is applied in the direction perpendicular to the interface.

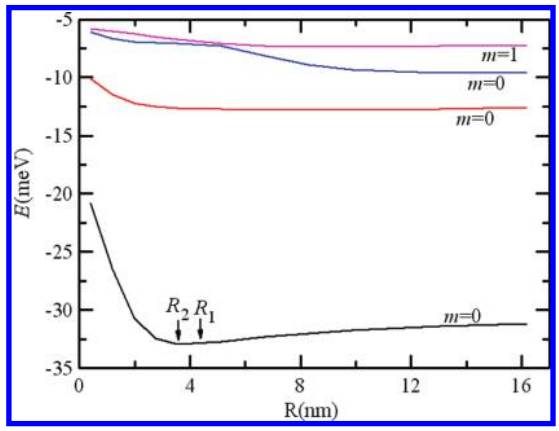

Figure 2. Energies of the five lowest states of a shallow donor impurity near the (001) surface of Si as a function of the distance, R, to the interface. The states are labeled by the value of the magnetic quantum number, m. The arrow indicates two values, $R_1 = 4.3$ nm and $R_2 = 3.6$ nm (see Figure 1) that were used in the results reported below for the two-donor case.

applied across the device is also relevant for quantum computation schemes. Coherent charge transport by adiabatic passage (CTAP) schemes have been proposed, but they require an array of three donors and the realization of time-dependent tunable barriers.[17]

The geometry of the device that we consider here is different from previous proposals[9,13] because the two donors are not placed at equal distance from the interface, in Figure 1, $R_1 \neq R_2$. Since the ionization potential of the dopant atom is controlled by its distance to the interface (see Figure 2), this gives us the ability to build a "heteronuclear" dopant molecule, and in principle to control the degree of covalent vs ionic bonding, using dopant atoms of the same chemical nature, here phosphorus. This flexibility is important for the design of logic schemes.

The conduction band of silicon has six equivalent minima located near the boundaries of the first Brillouin zone in the six (001) directions. Symmetry breaking at the site of the dopant atom leads to valley−orbit (VO) coupling and lifts the degeneracy of the ground state that is predicted by the single-valley formulation of effective mass theory.[18] More refined treatments that include the valley−orbit coupling have been proposed at the effective mass theory level[19] and beyond it, at the tight-binding[20] and atomic computational levels.[21]

Computational studies[19d,20d,e] of the field strength effects on the spectroscopy of a single dopant atom that include VO coupling show that in the case of a bulk-like donor far from the interface and for field strengths up to ≈20 kV/cm applied perpendicularly to the interface, the splitting between the ground state of A_1 symmetry and the triplet (T_2) and doublet (E_1) components remains essentially unchanged and equal to the zero field values (≈11.7 and 12.9 meV, respectively), in agreement with recent experimental results in the low[22] and high[5] field limits. Field effects are not found to be stronger for donors closer to the interface.[20e] As shown below, the field strengths required for charge switching between the two weakly coupled donors are ≈0.01 kV/cm when the field is applied parallel to the interface (see Figure 4 below) and 0.5 kV/cm when it is applied perpendicular to it (see Supporting Information, Figure S4). These field strengths will therefore not induce coupling between the GS of the dopants and the higher energy states of the manifold. They only couple the two GS of the pair of dopant atoms leading to a ground and an excited molecular electronic state. For this reason, we use below the single-valley approximation since it allows us to capture the essential physical aspects of the formation of the two lowest energy states of the molecular ion, made from the linear combination of the GS states of the two dopants. These are the electronic states used to implement the logic scheme for a full addition.

In the single-valley approximation the time-dependent Hamiltonian for N dopants written in Cartesian coordinates reads

$$H(t) = -\left[\frac{\hbar^2}{2m_\perp}\left(\frac{\partial^2}{\partial x^2} + \frac{\partial^2}{\partial y^2}\right) + \frac{\hbar^2}{2m_\parallel}\frac{\partial^2}{\partial z^2}\right] + e\mathbf{F}(t)\cdot r - \sum_{i=1}^{N}\frac{e^2}{\varepsilon_{Si}\sqrt{(x - x_i)^2 + y^2 + (z - z_i)^2}} + \sum_{i=1}^{N}\frac{Qe^2}{\varepsilon_{Si}\sqrt{(x - x_i)^2 + y^2 + (z - z_i)^2}} - \frac{Qe^2}{4\varepsilon_{Si}z} \quad (1)$$

where the first term is the kinetic energy of the electron, the second is the time-dependent external electric field potential, the third is the Coulomb potential of the two centers, and the fourth and the last are the image-charge potential of the donors and of the electron. $m_\perp = 0.191m_e$ and $m_\parallel = 0.916m_e$ (m_e is the mass of a free electron) are the transverse and longitudinal effective masses, respectively, and N is the number of donors. In the logic device that we discuss below, there are $N = 2$ dopants. $Q = (\varepsilon_{SiO_2} - \varepsilon_{Si})/(\varepsilon_{SiO_2} + \varepsilon_{Si})$ where $\varepsilon_{Si} = 11.4$ and $\varepsilon_{SiO_2} = 3.8$.[23a,b] The ground state and lowest excited state wave functions at zero and finite fields are solved numerically on a grid by the Lanczos method.[24] More details about the numerical method can be found in section 1 of the Supporting Information.

We first consider a single donor ($N = 1$) in the absence of an electric field. The results will serve as a basis for discussing the two-center ($N = 2$) case. The donor is located at a distance R from the interface and Figure 2 shows the five lowest eigenenergies as a function of R. Our results are consistent with those of ref 23a, where the energies were obtained by a variational method. For the one dopant case, the system is cylindrically symmetric and therefore the magnetic number m is a good quantum number. In Figure 2, the three lowest states (from bottom to upper) labeled by $m = 0$ correspond to the 1s, $2p_z$, and 2s orbitals of a hydrogen atom, and the states labeled by $m = 1$ are doubly degenerate, corresponding to the $2p_x$ and $2p_y$ orbitals.

We now consider the two-donor case with a single electron. Figure 3 shows the charge distribution of the ground and first excited states of the two-donor molecule in the $x-z$ plane when no external field is applied. The two dopants are located in the (x, z) plane and 32 nm apart along the x direction (see Figure 1), where $d = |x_2 - x_1|$. They are placed respectively at $R_1(=z_1)$

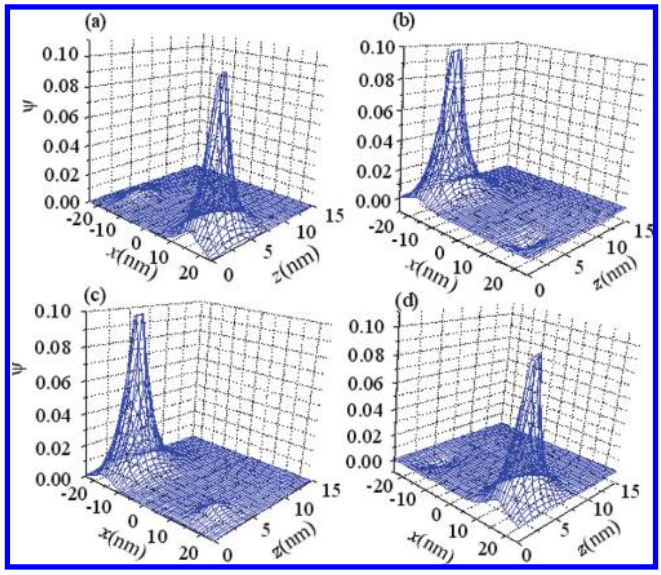

Figure 3. Amplitude wave function $\Psi(x, y, z)$ of the two lowest states of the dopant molecule in the xz ($y = 0$) plane for $F_x = 0$ (top) and $F_x = 0.01$ kV/cm (bottom). The left panels (a, c) show the ground state while the right panels (b, d) show the first excited state. At zero field, the ground state has an electron localized on the right, L^+R, while for the first excited state, the electron is localized on the left (LR^+). In the bottom panels, the applied field is sufficient to reverse the localization of the electron. The ground state (left, panel c) is now of the type LR^+, with the electron localized on the left, while the excited state has the electron localized on the right (L^+R).

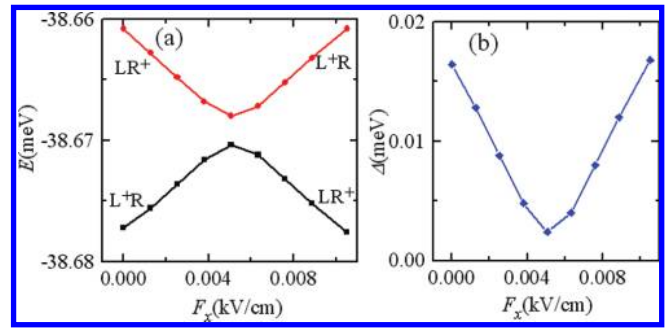

Figure 4. (a) Ground state and the first excited energies of a single electron bound to a shallow-donor pair as a function of the electric field strength (in kV/cm) applied in the x direction. Here L^+R means that the wave function of the electron is localized at the right donor while LR^+ means that the wave function is localized at the left donor. (b) Gap between the two states, Δ (meV), as a function of the field strength. See Figure S4 of the Supporting Information for similar results when the field is applied along the z direction.

$= 4.3$ nm (left) and R_2 ($=z_2$) $= 3.6$ nm (right) from the interface located at $z = 0$. The energy difference between the two ground states of the uncoupled dopants is about 0.015 meV. Because of the large distance between them ($d = 32$ nm), the two dopants are very weakly coupled. Therefore, by placing them at a slightly different distance from the interface, it is possible to almost completely localize the electron on the left or on the right in the ground state of the two-donor molecule, without applying any external field. From Figure 2, we see that $R_2 = 3.6$ nm, which defines the distance to the interface for the right dopant, corresponds to a lower energy than for the left dopant, placed at $R_1 = 4.3$ nm from the interface. Therefore, the electron is localized on the right dopant atom (positive x coordinate), as shown in Figure 3a. The hole is then on the dopant on the left. We denote the ground state of the one electron two dopant molecule as L^+R. The opposite is the case for the first excited state (panel b) that is denoted LR^+. Since the two dopants are chosen to be very far apart, the interdopant coupling is small. The energy gap between the two lowest states, $\Delta_0 \approx 0.016$ meV, is only slightly larger than that between the two isolated dopants and mainly controlled by the relative distance ($R_2 - R_1$) of the two donors to the interface. The control of the value of Δ_0 relies on the ability to precisely position the dopants at the sub nanometer scale and there are intensive research efforts in this direction using both top-down[25] and bottom-up dopant engineering.[2d,26] Recent theoretical simulation carried out at the effective mass approximation level including the valley-orbit coupling show that the field free exchange coupling between the two donors oscillates as a function of the interdonor distance due to the valley interference, in the case of both homo-[27] and heteronuclear[28] donor pairs. These oscillations are particularly important at short interdonor distances, comparable to the effective Bohr radius of the dopant atom. For the large interdonor distances considered here ($d = 32$ nm which is about 25 times the Bohr radius of the P atom), these oscillations are damped and are not expected to play an important role. The same authors showed that taking into account the VO coupling does not lead to oscillations of the interdopant coupling as a function of field strength.

3. Electric Field Induced Electron Transfer

The electron charge distribution can be shifted by applying a static electric field. This is shown in the two bottom panels (c and d) of Figure 3 computed for a field applied parallel to the interface, along the x direction, $F_x = 0.01$ kV/cm. The finite field value causes a reversal of the charge distribution, as seen by comparing the top and the bottom panels of Figure 3.

The reversal of the polarity of the charge orientation with the field applied in the x direction is shown vs the field strength in Figure 4. In Figure 4a, the energies of the ground and first excited states are plotted as a function of F_x (in kV/cm) while the gap between the two states is shown in panel b. The maximum energy gap, $\Delta_0 = 0.016$ meV, occurs at 0 and 0.01 kV/cm field strengths and is governed mainly by the position of the two donors with respect to the interface (see Figure 1). The minimum gap, $\Delta_{min} \approx 0.0024$ meV occurs when the two levels anti cross, for $F_x = 0.005$ kV/cm. This value is determined primarily by the lateral distance d between the two centers. The two energy gaps set the time limits of the proposed operation for the logic machine. In particular, the minimum gap, Δ_{min}, determines how fast a diabatic transition (meaning a curve crossing in panel a of Figure 4, e.g., L^+R to L^+R) must be for a diabatic state to be maintained as the field is changing. Here, as in other contexts (see, e.g., ref 29), by a diabatic state we mean a state with a definite configuration of the electrons. To ensure a clear difference between the adiabatic and the diabatic charge transfer, the value of the maximum energy gap Δ_0 must be large compared to Δ_{min}.

An adiabatic transition means that the quantum state is maintained and so the field change needs to be done slowly, and slower than h/Δ_{min}. A diabatic transition requires that the field is swept across the gap between the two adiabatic states in a time shorter than h/Δ_{min}; see, e.g., ref 29. The faster the diabatic switching, the better the localization of the electron on a given site is preserved. Since one cannot currently switch an electric field in much less than 100 ps, following a diabatic path requires a minimal gap, Δ_{min}, much smaller than 0.04 meV.

To design a practical logic scheme, one has also to take into account the stability of the states of the donor molecule with respect to phonon coupling strength. The latter varies exponen-

tially with the distance, d, between the two donors.[2b,9] From the prediction of ref 9, we estimate that for a distance d of 32 nm, the T_1 lifetime of the states is about 1 ms, which is much longer than the time of operation of the machine discussed below. This theoretically predicted value has been experimentally verified[2b] for the system we propose. This time corresponds to the relaxation time of states of the donor pair and is much longer than the orbital relaxation time measured for donor atoms in bulk in optical experiments, which are of the order of picoseconds.[30] The time scale for the charge decoherence is discussed in section 5 below.

Finally, we note that even though all the excited states are included in the Lanczos procedure, it is possible to summarize the essence of the results shown in Figures 3 and 4 by a two state model. This model is discussed in more detail in section 2 of the Supporting Information.

The implementation of the full adder logic makes essential use of our ability to control the electron localization by the electric field.

To address or to change the state of the two-center system, we use a time dependent electrical field. We describe the action of the field by solving the time-dependent Schrödinger equation, $i\hbar\, d\Psi(\mathbf{n};t)/dt = H(\mathbf{n},t)\,\Psi(\mathbf{n};t)$, on a grid using a fourth-order Runge−Kutta method.[31] $\mathbf{n}$ designates a grid point in three dimensions. We consider a field parallel to the interface, in the x direction. Such a field is roughly parallel to the line of centers of the two dopants. It is therefore better able to control the charge. Experimentally one can also apply a field perpendicular to the interface. We show in the Supporting Information, section 4, that diabatic and adiabatic charge transfers can also be implemented in such a configuration, but that this requires larger field strengths than the one used for a field applied parallel to the interface.

In any one cycle of the logic device we take an electric field given by

$$F_x(t) = \begin{cases} F_{\max} \exp(-(t - t_{on})^2/2t_w^2) & t \le t_{on} \\ F_{\max} & t_{on} < t \le t_{off} \\ F_{\max} \exp(-(t - t_{off})^2/2t_w'^2) & t > t_{off} \end{cases} \quad (2)$$

The important parameter is the duration of the pulse that is determined by the value of the widths, t_w and t_w' for switching the field on and off, respectively. Electrical addressing of nanosized logic devices can nowadays be switched on or off at the 100 GHz scale. We need to be able to switch the field off in either an adiabatic or a sudden fashion. The boundary between these two regimes is determined by the minimal splitting of the levels, as shown in Figure 4. For realistic geometries it will better if the switching off time can be brought down to a few dozen picoseconds or even shorter.

For a field parallel to the surface, we took F_{max} to be 0.01 kV/cm (see Figure 4). When the field is applied in the direction perpendicular to the interface, see Figure S4 of Supporting Information, the value of F_{max} is 0.47 kV/cm.

We define the charge densities on the two donors, ρ_L and ρ_R, by dividing the system into two regions: a left region ($x < 0$) containing the left donor and a right region ($x > 0$) that contains the right donor. Then the charge density on the left is computed as $\rho_L(t) = \sum_{i,j,k}|\Psi(i,j,k;t)|^2$, where the sum is over all the grid points in the left region, and $\rho_R(t)$ is defined in a similar way. The behavior of the charge densities can be understood from Figure 4 and is shown in Figure 5 for an adiabatic switching

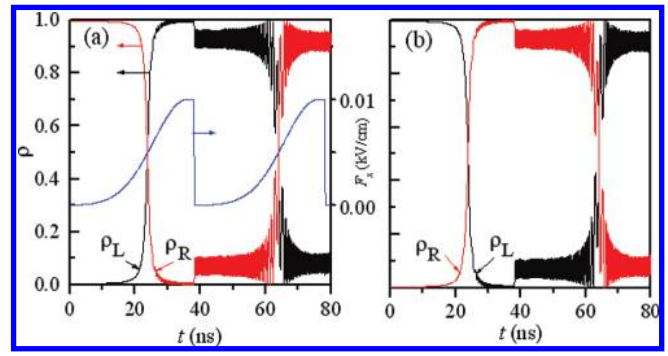

Figure 5. Computed charge densities on the left and on the right dopants, ρ_L and ρ_R, as a sequence of two pulses is applied to the two donor pair. The total duration of one pulse is 40 ns. The shape of the pulse is given by eq 2 and its time dependent strength is shown on the left ordinate axis of panel (a) (blue). $t_{on} = 36$ ns, $t_{off} = 38$ ns, $t_w = 10$ ns, and $t_w' = 100$ ps. $F_{max} = 0.01$ kV/cm. In (a), the initial condition is the ground state when $F_x = 0$. In (b), the initial condition is the first excited state when $F_x = 0$. See Supporting Information, Figure S2, for the results with a faster switching off constant, $t_w' = 20$ ps.

constant, $t_w = 10$ ns, and a diabatic switching off constant, t_w' = 100 ps (see eq 2). These switching times ensure that the switching-on process ($t < t_{on}$) of the electric field is long so that it is an adiabatic process where the quantum state of the system is maintained, as can be seen in Figure 5. Say that the system is initially in the absence of the field in the ground state; cf. Figure 5a. Then the electron is localized around the right donor. By adiabatically switching on the electric field, we move the electron from the right donor to the left, that is, from state L^+R to LR^+. In such a process the system stays in the ground state, meaning that its energy follows the lower curve in Figure 4. The quantum state is preserved even though the electron has switched sides. Next, at t_{off}, we suddenly switch off the field very fast. The system has little time to adjust to this change and continues to stay at essentially the same state of the electron, namely, LR^+. Since this state is not an exact eigenstate of the Hamiltonian at the final stage (when $F_x = 0$), the charge density oscillates with a small amplitude around a mean value that is not exactly 1 or 0. The oscillation period is governed by Δ_0 (see the Supporting Information for an analytical derivation on the 2 × 2 model) and the mean values of the charge on the left and on the right depends on how fast we switch off the electric field. This point is further illustrated in the Supporting Information (see in particular Figure S2) where faster values of the switching off time, t_w', are considered.

The net effect after one cycle, duration 40 ns in Figure 5, is that the electron is moved from a zero field state L^+R to a zero field excited state LR^+, going through the intermediate state LR^+ at finite field. This intermediate state is actually the ground state of the system when the field is on. In Figure 5b, we show the complementary situation, where the initial state at zero field is the excited state of the donor pair, localized on the left donor.

When a second pulse is applied, we necessarily start from the first excited state at $F = 0$ (panel a). If we adiabatically switch on the electric field again as before, the system follows the upper curve in Figure 4. Then, as we suddenly switch the field off, the system goes back to the zero field initial state, the ground state L^+R. Therefore, we can shift the electron between the left and the right donors by applying the electric field pulse sequence given by eq 2. This is shown schematically in the table of contents figure.

When we choose a switching off time constant t_w' experimentally realistic as in the simulation shown in Figure 5, the

TABLE 1: Operation of the First Half Adder That Realizes the Addition of the "Carry in" and of One of the Input Digits[a]

initial state	voltage pulse	intermediate state = intermediate sum = output of XOR	output of AND operation (C_1) = charge on right dopant R at F_{max}	output of INHibit = charge on Left dopant at F_{max}
L^+R (0)	0	L^+R (0)	0	0
L^+R (0)	1	LR^+ (1)	0	1
LR^+ (1)	0	LR^+ (1)	0	0
LR^+ (1)	1	L^+R (0)	1	0

[a] The initial state, left column, is the state of the machine that stores the "carry in". The value of the "carry in" is shown as the argument. A logical value of 0 for the carry is encoded on the state L^+R where the electron is localized on the right dopant at zero field while a logical value 1 is encoded in the state LR^+ where the electron is localized on the left dopant at zero field. The voltage is not or is applied depending on the value of the bit, 0 or 1, to be added. (The state of the machine is read at the end of the pulse when the field is zero). The eXclusive OR (or XOR) operation is the intermediate sum. The charge on the left or on the right dopant as given in the last two columns is measured at the plateau of the field strength where the field is maximal. For a half addition it is sufficient to read the charge on the dopant on the right. The table also shows that the measure of the charge on the left dopant at high field corresponds to an inhibit, INH, operation, which enables us to implement a half subtraction in parallel with the half addition.

TABLE 2: Operation of the Second Half Adder That Realizes the Addition of the Intermediate Sum and of the Second of the Input Digits[a]

intermediate state = intermediate sum	voltage pulse	final state = sum out	charge on R at F_{max} = output of AND (C_2)	charge on L at F_{max} = output of INH
L^+R (0)	0	L^+R (0)	0	0
L^+R (0)	1	LR^+ (1)	0	1
LR^+ (1)	0	LR^+ (1)	0	0
LR^+ (1)	1	L^+R (0)	1	0

[a] The state of the machine is always defined at zero field. The charge on the left and right dopant is measured at the maximum field strength.

fact that the switching off of the pulse is not perfectly diabatic prevents a complete charge transfer when a second pulse is applied. The faster the switching off, the more complete is the charge transfer (see Supporting Information for a simulation with faster t'_w). For a 100 ps switching off time, the localization of the charge after the second pulse is still about 90%.

4. Logic Scheme for a Full Addition

The logical operations of the full adder are performed physically by the slow rise and rapid decrease of the applied voltage pulse that corresponds to an adiabatic and diabatic electron transfer between the two donors, as discussed above and summarized in the table of contents figure.

The full adder operates as a finite state machine. We use four internal states of the machine: two levels at zero field and two at a finite gate field. The two levels at zero gate are the ground state L^+R (electron localized on the right) and the first excited state LR^+ (electron on the left) while at finite high field the ground state is LR^+ (electron on the left) and the first excited state is L^+R (electron localized on the right); see Figure 4.

A full addition is a logic operation with three inputs, a "carry in" digit that comes from the previous addition and two input digits that need to be added. The addition has two outputs, a "sum out" that is the digit representing addition modulo 2 of the two input digits and the "carry out" that becomes the "carry in" for the next addition.

We store the "carry in" bit in an internal state of the machine at zero field. We take that the electron on the right, that is L^+R, corresponds to the logic value 0, while the electron on the left, that is LR^+, corresponds to the logic value 1. For the machine to be cyclable it is necessary that at the end of the addition the "carry out" digit is stored as an internal state of the machine, ready to be used as the "carry in" bit for the next addition.

The first digit to be added is encoded in applying or not a voltage pulse. If the digit to be added has logical value 0, no pulse is applied while if the digit has the value 1, a pulse is applied. The shape of the pulse is given in eq 2. As discussed above, it is such that it induces an adiabatic electron transfer between the two dopants when it rises and because it is switched off diabatically, the localization of the electron is preserved when the electric field goes back to zero.

The localization of the electron is changed from left to right or vice versa when the pulse field is applied, rows 2 and 4 in Table 1, which performs a XOR (or addition modulo 2) operation between the input and the state of the machine. The intermediate carry output is encoded into the localization of the electron on the right dopant at high field, before it is diabatically switched off. If the electron is localized on the right dopant at high field during the pulse, the intermediate carry has logical value 1 and if not, it has logical value 0. The measure of the charge of the right dopant at high field corresponds to the AND operation between the input digit and the state of the machine and gives the intermediate carry. This intermediate carry is only one when the carry in value is one and the pulse is applied (logical value of the input is 1). This corresponds to row 4 of Table 1.

The full addition proceeds in two cycles. During the first cycle, the device performs the half addition of the "carry in" digit, which is already in its memory and one of the inputs. This intermediate cycle leads to an "intermediate carry out" and an "intermediate sum". The operations are summarized in the traditional form for logic, namely a "transition table", in Table 1.

At the end of the first half addition, the intermediate sum is stored as the state of the machine and the first carry output, C_1, has been measured at the high field plateau. In the second half addition, Table 2, the second input digit is added to the intermediate sum, leading to the sum out and the second carry C_2. The sum out is the state of the machine at zero field, after the second pulse is over. The C_2 output is given by the value, 0 or 1, of the charge on the right dopant at high field. Since the two carries, C_1 and C_2, cannot be 1 simultaneously, to detect a

charge on the right dopant at high field during either one of the two cycles means that the carry out is 1.

5. Considerations on the Experimental Realization of the Full Adder Logic Scheme

The full adder logic scheme discussed above can be experimentally realized by integrating the two donor system with a single electron transistor (RF-SET) and a pulse gate. It has been shown that this experimental setup allows for fast electrical readout and control of the double donor charge state.[2b] SETs operating at radio frequencies (RF-SETs) are proven to be fast and highly sensitive charge detectors, allowing electrometry with subelectron resolution down to the quantum limit.[32] Charge sensitivities of 10 $\mu e/Hz^{1/2}$ at megahertz bandwidth were demonstrated using silicon RF-SETs.[33] The entire gate pulse sequence for a full adder requires three pulses, which rise adiabatically and fall suddenly. The first pulse sets the system in its initial state, depending on the carry-in value. The next two pulses correspond to the logic inputs and are kept at F_{max} for a time long enough (approximately microseconds) for the RF-SET to measure whether the charge is on the right dopant. After these pulses are applied, the final state of the system, that is the sum, is read out by the RF-SET. To reset the system to the ground state, the electron is first drained to a nearby decoupled reservoir by applying a field pulse. Then an electron is loaded to the right dopant by increasing the coupling between the reservoir and the double donor system. This reset procedure will return the system to the ground state of the donor pair at zero field, whether the final state was the ground or the excited state.

The total length of a pulse sequence is much shorter than the computed phonon decoherence lifetime of the system,[2b,9] which was experimentally verified in ref 2b. We assume that the duration of the sequence of three pulses is also shorter than the charge decoherence time, τ_ϕ. An upper limit for the dephasing time of ~720 ns was calculated using the Johnson formula for an electron temperature of 10 K.[34] Charge decoherence times of ~1 ns measured in GaAs double quantum dots[35] can be taken as a lower limit.

Temperature is an important parameter as it influences both relaxation and dephasing rates. The relaxation T_1 time of 1 ms we refer to above was measured for two phosphorus donors 50 nm apart at a phonon temperature, T_{ph}, of 50 mK in a dilution refrigerator[2b] and is in agreement with the predictions of ref 9, which are based on a model that considers phonon emission with a T_{ph} of 100 mK. It is important to note that T_{ph} is much lower than the electronic noise temperature (10 K) used to calculate the charge decoherence time of $\tau_\phi \sim 720$ ns discussed above.[34] At zero electric field, the energy gap between the right and left state corresponds to a temperature of 200 mK. Similarly, the energy gap between the left and right state at $F_x \sim 0.008$ kV/cm is 200 mK.

The proposed protocol does not have 100% fidelity, due to delocalization of the wave function after each diabatic fall off of the pulse. The parameters of the donor pair were set for this fall off to be compatible with a voltage switching rate of 100 GHz. The fidelity could be improved by using faster diabatic switching rates, and we show an example in the Supporting Information (Figure S2). Even if the complete pulse sequence is carried out in a time shorter than the charge decoherence time, the projective measurements performed after each pulse will lead to a 10% chance of the wave function collapsing to the undesired state and require more than one measurement. Three pulses would lead to fidelity of 73%. One way to improve the fidelity is to initialize the system in the state corresponding to the carry in digit by using a high field strength, which will localize the electron either on the left or on the right by increasing the energy gap Δ between the two states (see Figure 4). If one further checks whether the state is initialized correctly by measuring the charge state, the cycle always starts from a purely left or right state, which increases the fidelity to 80%. After each full addition, the system is reset to the ground state, so there is no further degradation of the fidelity.

6. Conclusion

We show that it is possible to implement a full adder by controlling electron localization with voltage pulses in the two lowest excited states of a donor pair molecule. Time-dependent simulations based on the effective mass model for the donor molecule support the proposed logic scheme, which can realized on a CMOS compatible device, using realistic switching and acquisition times and a RF-SET for charge detection.

Acknowledgment. This work was supported by the FP7 FET proactive NANO-ICT project MOLOC (215750).

Supporting Information Available: Additional details on the numerical methods used for integrating the time-dependent Schroedinger equation on a grid and on the analysis of the numercial results using a 2×2 Hamiltonian model, as well as additional results for an external field applied perpendicular to the interface. This material is available free of charge via the Internet at http://pubs.acs.org.

References and Notes

(1) (a) Heath, J. R.; Ratner, M. A. Molecular electronics. *Phys. Today* **2003**, *56* (5), 43–49. (b) deSilva, A. P. Molecular computation - Molecular logic gets loaded. *Nat. Mat.* **2005**, *4* (1), 15–16. (c) Baron, R.; Lioubashevski, O.; Katz, E.; Niazov, T.; Willner, I. Elementary arithmetic operations by enzymes: A model for metabolic pathway based computing. *Angew. Chem., Int. Ed.* **2006**, *45* (10), 1572–1576. (d) Margulies, D.; Melman, G.; Shanzer, A. A molecular full-adder and full-subtractor, an additional step toward a moleculator. *J. Am. Chem. Soc.* **2006**, *128* (14), 4865–4871. (e) Raymo, F. M.; Tomasulo, M. Optical processing with photochromic switches. *Chem.—Eur. J.* **2006**, *12* (12), 3186–3193. (f) Balzani, V.; Credi, A.; Venturi, M. *Molecular Devices and Machines. A Journey into the Nano World.*: Wiley-VCH: Weinheim, 2008; (g) Duchemin, I.; Renaud, N.; Joachim, C. An intramolecular digital 1/2-adder with tunneling current drive and read-outs. *Chem. Phys. Lett.* **2008**, *452*, 269–274. (h) Waser, R. *Information Technology IV*; Wiley: Weinheim, 2008; Vol. 4, p 213−248. (i) Szacilowski, K. Digital information processing in molecular systems. *Chem. Rev.* **2008**, *108* (9), 3481–3548. (j) de Ruiter, G.; Tartakovsky, E.; Oded, N.; van der Boom, M. E. Sequential Logic Operations with Surface-Confined Polypyridyl Complexes Displaying Molecular Random Access Memory Features. *Angew. Chem., Int. Ed.* **2009**, *49* (1), 169–172. (k) Heath, J. R. Molecular Electronics. *Annu. Rev. Mater. Chem.* **2009**, *39*, 1–23. (l) Andreasson, J.; Pischel, U. Smart molecules at work-mimicking advanced logic operations. *Chem. Soc. Rev.* **2010**, *39* (1), 174–188.

(2) (a) Rueb, F. J.; Pok, W.; Reusch, T. C. G.; Butcher, M. J.; Goh, K. E. J.; Oberbeck, L.; Scappucci, G.; Hamilton, A. R.; Simmons, M. Y. Realization of atomically controlled dopant devices in silicon. *Small* **2007**, *3* (4), 563–567. (b) Andresen, S. E. S.; Brenner, R.; Wellard, C. J.; Yang, C.; Hopf, T.; Escott, C. C.; Clark, R. G.; Dzurak, A. S.; Jamieson, D. N.; Hollenberg, L. C. L. Charge State Control and Relaxation in an Atomically Doped Silicon Device. *Nano Lett.* **2007**, *7* (7), 2000–2003. (c) Weis, C. D.; Schuh, A.; Batra, A.; Persaud, A.; Rangelow, I. W.; Bokor, J.; Lo, C. C.; Cabrini, S.; Sideras-Haddad, E.; Fuchs, G. D.; Hanson, R.; Awschalom, D. D.; Schenkel, T. Single atom doping for quantum device development in diamond and silicon. *J. Vac. Sci. Technol.* **2008**, *26* (6), 2596–2600. (d) Fuechsle, M.; MahapatraS; Zwanenburg, F. A.; Friesen, M.; Eriksson, M. A.; Simmons, M. Y. Spectroscopy of few-electron single-crystal silicon quantum dots. *Nat. Nano* **2010**, *5* (7), 502–505.

(3) Sellier, H.; Lansbergen, G. P.; Caro, J.; Rogge, S.; Collaert, N.; Ferain, I.; Jurczak, M.; Biesemans, S. Transport Spectroscopy of a Single Dopant in a Gated Silicon Nanowire. *Phys. Rev. Lett.* **2006**, *97* (20), 206805–4.

(4) Klein, M.; Lansbergen, G. P.; Mol, J. A.; Rogge, S.; Levine, R. D.; Remacle, F. Reconfigurable Logic Devices on a Single Dopant Atom up to a Full Adder by Electrical Spectroscopy. *ChemPhysChem.* **2009**, *10*, 162–173.

(5) Lansbergen, G. P.; Rahman, R.; Wellard, C. J.; Woo, I.; Caro, J.; Collaert, N.; Biesemans, S.; Klimeck, G.; Hollenberg, L. C. L.; Rogge, S. Gate-induced quantum confinement transition of a single dopant atom in a silicon FinFET. *Nature Physics* **2008**, *4*, 656–661.

(6) Kohavi, Z. *Switching and Finite Automata Theory*; Tata McGraw-Hill: New Delhi, 1999.

(7) (a) Remacle, F.; Levine, R. D. All Optical Digital Logic: Full Addition or Subtraction on a Three-State System. *Phys. Rev. A* **2006**, *73*, 033820−7. (b) Remacle, F.; Speiser, S.; Levine, R. D. Intermolecular and Intramolecular Logic Gates. *J. Phys. Chem. B* **2001**, *105*, 5589–5591.

(8) (a) Kuznetz, O.; Salman, H.; Eichen, Y.; Remacle, F.; Levine, R. D.; Speiser, S. All optical Full-adder Based on Intramolecular Electronic Energy transfer in the Rhodamine-Azulene Bichromophoric system. *J. Phys. Chem. C* **2008**, *112*, 15880–15885. (b) Remacle, F.; Weinkauf, R.; Levine, R. D. Molecule-Based Photonically-Switched Half and Full Adder. *J. Phys. Chem. A* **2006**, *110* (1), 177–184.

(9) Barrett, S. D.; Milburn, G. J. Measuring the decoherence rate in a semiconductor charge qubit. *Phys. Rev. B* **2003**, *68* (15), 155307.

(10) Vitanov, N. V.; Halfmann, T.; Shore, B. W.; Bergmann, K. Laser-induced Population Transfer by Adiabatic Passage Technique. *Annu. Rev. Phys. Chem.* **2001**, *52*, 763–809.

(11) (a) Remacle, F.; Heath, J. R.; Levine, R. D. Electrical Addressing of Confined Quantum Systems for Quasiclassical Computation and Finite State Logic Machines. *Proc. Natl. Acad. Sci. U.S.A.* **2005**, *102*, 5653–5658. (b) Remacle, F.; Levine, R. D. Towards Molecular Logic Machines. *J. Chem. Phys.* **2001**, *114* (23), 10239–10246.

(12) (a) Klein, M.; Rogge, S.; Remacle, F.; Levine, R. D. Transcending binary logic by gating three coupled quantum dots. *Nano Lett.* **2007**, *7*, 2795–2799. (b) Medalsy, I.; Klein, M.; Heyman, A.; Shoseyov, O.; Remacle, F.; Levine, R. D.; Porath, D. Logic Implementations at the Nanoscale Using a Single Nanoparticle-Protein Hybrid: Boolean and Beyond Boolean Finite State Machines. *Nat. Nano* **2010**, *5*, 451–457. (c) Klein, M.; Mol, J. A.; Verduijn, J.; Lansbergen, G. P.; Rogge, S.; Levine, R. D.; Remacle, F. Ternary Logic Implemented on a Single Dopant Atom FET in Si. *Appl. Phys. Lett.* **2010**, *96*, 043107.

(13) (a) Wellard, C. J.; Hollenberg, L. C. L.; Das Sarma, S. Theory of the microwave spectroscopy of a phosphorus-donor charge qubit in silicon: Coherent control in the Si:P quantum-computer architecture. *Phys. Rev. B* **2006**, *74* (7), 075306−9. (b) Calderon, M. J.; Koiller, B.; Das Sarma, S. External field control of donor electron exchange at the Si/SiO_2 interface. *Phys. Rev. B* **2007**, *75* (12), 125311–11. (c) Calderon, M. J.; Koiller, B.; Das Sarma, S. Proposal for electron spin relaxation measurements using double-donor excited states in Si quantum computer architectures. *Phys. Rev. B* **2007**, *75* (16), 161304–4.

(14) Kane, B. E. A silicon-based nuclear spin quantum computer. *Nature* **1998**, *393* (6681), 133–137.

(15) (a) Petta, J. R.; Johnson, A. C.; Taylor, J. M.; Laird, E. A.; Yacoby, A.; Lukin, M. D.; Marcus, C. M.; Hanson, M. P.; Gossard, A. C. Coherent Manipulation of Coupled Electron Spins in Semiconductor Quantum Dots. *Science* **2005**, *309* (5744), 2180–2184. (b) Koppens, F. H. L.; Buizert, C.; Tielrooij, K. J.; Vink, I. T.; Nowack, K. C.; Meunier, T.; Kouwenhoven, L. P.; Vandersypen, L. M. K. Driven coherent oscillations of a single electron spin in a quantum dot. *Nature* **2006**, *442* (7104), 766–771.

(16) Hanson, R.; Kouwenhoven, L. P.; Petta, J. R.; Tarucha, S.; Vandersypen, L. M. K. Spins in few-electron quantum dots. *Rev. Mod. Phys.* **2007**, *79*, 1217–1265.

(17) (a) Cole, J. H.; Greentree, A. D.; Hollenberg, L. C. L.; Das Sarma, S. Spatial adiabatic passage in a realistic triple well structure. *Phys. Rev. B* **2008**, *77* (23), 235418–10. (b) Hollenberg, L. C. L.; Greentree, A. D.; Fowler, A. G.; Wellard, C. J. Two-dimensional architectures for donor-based quantum computing. *Phys. Rev. B* **2006**, *74* (4), 045311−8. (c) Rahman, R.; Park, S. H.; Cole, J. H.; Greentree, A. D.; Muller, R. P.; Klimeck, G.; Hollenberg, L. C. L. Atomistic simulations of adiabatic coherent electron transport in triple donor systems. *Phys. Rev. B* **2009**, *80* (3), 035302−7.

(18) Kohn, W. In *Solid State Physics-Advances in Research and Applications*; Seitz, F., Turnbull, D., Eds.; Academic Press: New York, 1957; Vol. 5, p 257.

(19) (a) Baldereschi, A. Valley-Orbit Interaction in Semiconductors. *Phys. Rev. B* **1970**, *1* (12), 4673. (b) Sham, L. J.; Nakayama, M. Effective-mass approximation in the presence of an interface. *Phys. Rev. B* **1979**, *20* (2), 734. (c) Friesen, M.; Chutia, S.; Tahan, C.; Coppersmith, S. N. Valley splitting theory of SiGe/Si/SiGe quantum wells. *Phys. Rev. B* **2007**, *75* (11), 115318–12. (d) Debernardi, A.; Baldereschi, A.; Fanciulli, M. Computation of the Stark effect in P impurity states in silicon. *Phys. Rev. B* **2006**, *74* (3), 035202.

(20) (a) Grosso, G.; Parravicini, G. P.; Piermarocchi, C. Valley splitting in triangular Si(001) quantum wells. *Phys. Rev. B* **1996**, *54* (23), 16393. (b) Martins, A. S.; Boykin, T. B.; Klimeck, G.; Koiller, B. Conduction-band tight-binding description for Si applied to P donors. *Phys. Rev. B* **2005**, *72* (19), 193204. (c) Boykin, T. B.; Klimeck, G.; Friesen, M.; Coppersmith, S. N.; von Allmen, P.; Oyafuso, F.; Lee, S. Valley splitting in low-density quantum-confined heterostructures studied using tight-binding models. *Phys. Rev. B* **2004**, *70* (16), 165325. (d) Rahman, R.; Wellard, C. J.; Bradbury, F. R.; Prada, M.; Cole, J. H.; Klimeck, G.; Hollenberg, L. C. L. High Precision Quantum Control of Single Donor Spins in Silicon. *Phys. Rev. Lett.* **2007**, *99* (3), 036403−4. (e) Rahman, R.; Lansbergen, G. P.; Park, S. H.; Verduijn, J.; Klimeck, G.; Rogge, S.; Hollenberg, L. C. L. Orbital Stark effect and quantum confinement transition of donors in silicon. *Phys. Rev. B* **2009**, *80* (16), 165314–10.

(21) Foreman, B. A. First-principles envelope-function theory for lattice-matched semiconductor heterostructures. *Phys. Rev. B* **2005**, *72* (16), 165345.

(22) Bradbury, F. R.; Tyryshkin, A. M.; Sabouret, G.; Bokor, J.; Schenkel, T.; Lyon, S. A. Stark Tuning of Donor Electron Spins in Silicon. *Phys. Rev. Lett.* **2006**, *97* (17), 176404.

(23) (a) MacMillen, D. B.; Landman, U. Variational solutions of simple quantum systems subject to variable boundary conditions. II. Shallow donor impurities near semiconductor interfaces: Si, Ge. *Phys. Rev. B* **1984**, *29* (8), 4524. (b) Calderon, M. J.; Koiller, B.; Hu, X.; Das Sarma, S. Quantum Control of Donor Electrons at the $Si-SiO_2$ Interface. *Phys. Rev. Lett.* **2006**, *96* (9), 096802−4.

(24) Cullum, J. K.; Willoughby, R. A. *Lanczos Algorithm for Large Symmetric Eigenvalues Computations*; Birkhauser: Boston, 1985.

(25) Andresen, S. E. S.; Brenner, R.; Wellard, C. J.; Yang, C.; Hopf, T.; Escott, C. C.; Clark, R. G.; Dzurak, A. S.; Jamieson, D. N.; Hollenberg, L. C. L. Charge State Control and Relaxation in an Atomically Doped Silicon Device. *Nano Lett.* **2007**, *7* (7), 2000–2003.

(26) Fuhrer, A.; Fuechsle, M.; Reusch, T. C. G.; Weber, B.; Simmons, M. Y. Atomic-Scale, All Epitaxial In-Plane Gated Donor Quantum Dot in Silicon. *Nano Lett.* **2009**, *9* (2), 707–710.

(27) Hu, X.; Koiller, B.; Das Sarma, S. Charge qubits in semiconductor quantum computer architecture: Tunnel coupling and decoherence. *Phys. Rev. B* **2005**, *71* (23), 235332.

(28) Koiller, B.; Hu, X.; Das Sarma, S. Electric-field driven donor-based charge qubits in semiconductors. *Phys. Rev. B* **2006**, *73* (4), 045319.

(29) Levine, R. D. *Molecular Reaction Dynamics*; Cambridge University Press: Cambridge, U.K., 2005.

(30) Vinh, N. Q.; Greenland, P. T.; Litvinenko, K.; Redlich, B.; van der Meer, A. F. G.; Lynch, S. A.; Warner, M.; Stoneham, A. M.; Aeppli, G.; Paul, D. J.; Pidgeon, C. R.; Murdin, B. N. Silicon as a model ion trap: Time domain measurements of donor Rydberg states. *Proc. Natl. Acad. Sci. U.S.A.* **2008**, *105* (31), 10649–10653.

(31) Press, W. H.; Teukolsky, S. A.; Vetterling, W. T.; Flannery, B. P. *Numerical Recipes*; Cambridge University Press: New York, 1992.

(32) Schoelkopf, R. J.; Wahlgren, P.; Kozhevnikov, A. A.; Delsing, P.; Prober, D. E. The Radio-Frequency Single-Electron Transistor (RF-SET): A Fast and Ultrasensitive Electrometer. *Science* **1998**, *280* (5367), 1238–1242.

(33) Angus, S. J.; Ferguson, A. J.; Dzurak, A. S.; Clark, R. G. A silicon radio-frequency single electron transistor. *Appl. Phys. Lett.* **2008**, *92* (11), 112103–3.

(34) Hollenberg, L. C. L.; Dzurak, A. S.; Wellard, C.; Hamilton, A. R.; Reilly, D. J.; Milburn, G. J.; Clark, R. G. Charge-based quantum computing using single donors in semiconductors. *Phys. Rev. B* **2004**, *69* (11), 113301.

(35) (a) Oosterkamp, T. H.; Fujisawa, T.; van der Wiel, W. G.; Ishibashi, K.; Hijman, R. V.; Tarucha, S.; Kouwenhoven, L. P. Microwave spectroscopy of a quantum-dot molecule. *Nature* **1998**, *395* (6705), 873–876. (b) Hayashi, T.; Fujisawa, T.; Cheong, H. D.; Jeong, Y. H.; Hirayama, Y. Coherent Manipulation of Electronic States in a Double Quantum Dot. *Phys. Rev. Lett.* **2003**, *91* (22), 226804.

JP103524D